Applied Catalysis B: Environmental 304 (2022) 120911

Contents lists available at ScienceDirect

Applied Catalysis B: Environmental

journal homepage: www.elsevier.com/locate/apcatb

Co-processing bio-liquids with vacuum gasoil through hydrocracking

Donia Bouzouita [a], Aleksandra Lelevic [a,b], Chantal Lorentz [a], Robbie Venderbosch [c], Thomas H. Pedersen [d], Christophe Geantet [a,*], Yves Schuurman [a,*]

[a] Univ Lyon, Université Claude Bernard Lyon 1, CNRS, IRCELYON UMR 5256, F-69626 Villeurbanne, France
[b] IFP Energies nouvelles, Rond-point de l'échangeur de Solaize BP 3, 69360 Solaize, France
[c] BTG Biomass Technology Group, Enschede, The Netherlands
[d] Department of Energy Technology, Aalborg University, Pontoppidanstræde 111, 9220 Aalborg Øst, Denmark

ARTICLE INFO

Keywords:
Bifunctional catalysis
Biofuels
Pyrolysis oil
Hydrothermal liquefaction
Middle distillates

ABSTRACT

Hydrocracking converts heavy feeds mainly into middle distillate products. Co-processing these bio-feeds with vacuum gas oil is a possible production route for biofuels. Stabilized bio-liquid from fast pyrolysis and hydrothermal liquefaction bio-crude were mixed with vacuum gas oil (10–20 wt%) and hydrocracked over a bifunctional catalyst. The impact of the bio-liquids on conversion and middle distillate selectivity were investigated. The liquid products were analyzed by several methods such as 2-dimensional gas chromatography coupled with simulated distillation to obtain quantitative distribution of monoaromatics, polyaromatics and saturated hydrocarbons. A quantification study of different types of carbons was performed by ^{13}C NMR and showed the evolution of products. The nature of bio-liquid impacts slightly on the conversion and gas production but not on the selectivity of middle distillates and naphtha. This is explained by a decoupled hydrodeoxygenation and hydrocracking process. This also resulted in a high hydrodesulfurization conversion.

1. Introduction

Among the various pathways for upgrading bio-liquids issued from thermochemical processes such as fast pyrolysis (FP) or hydrothermal liquefaction (HTL), co-processing in existing oil refinery units appears to be an eco-efficient, minimizing ecological impacts while maximizing the economics, and technically viable solution [1–3]. However, the introduction of bio-compounds should not affect the performance of the catalysts and maintain the quality of the final products such as the sulfur content for HDS (Hydrodesulfurization) or product distribution for FCC (Fluid Catalytic Cracking) or hydrocracking. Typically, the objective is to introduce 1–10 wt% of bio-liquids in the process.

Co-processing of FP bio-liquids through FCC has been investigated more than co-hydrocracking. For example Bezergianni et al. [4] reviewed a number of co-FCC studies, from laboratory to demo scale. FCC requires high reaction temperatures (500–600 °C) and favors the cracking of the bio-liquid simultaneously with deoxygenation due to hydrogen transfer from the hydrocarbon feedstock, even if some oxygenated molecules were observed in the final products [5]. Literature demonstrates the strong potential of this technology, up to 20 wt% of FP bio-liquid [3–6]. Co- processing of HTL bio-crude in FCC was also investigated [7].

Catalytic hydrocracking, performed under hydrogen pressure, is combining sulfide catalysts and acidic zeolites (or amorphous silica alumina's) to provide refiners a way to produce mostly middle distillates from heavy feeds ranging from vacuum gasoil (VGO) to vacuum residue [8–11]. In fact, hydrocracking refers to a wide range of processes ranging from mild hydrocracking [10] and conventional hydrocracking in fixed bed reactors to deep hydrocracking with slurry [12] or ebullated bed reactors [13]. It is a flexible process regarding the feedstocks, since it can convert viscous feeds containing long chains, aromatic and polyaromatic compounds and remove heterogeneous compounds such as S, N or metals (Ni, V) or O when bio-liquids are introduced. In terms of viscosity, the bio-liquids obtained from FP or HTL can be compared to vacuum distillation products and their reactivity was found to require rather harsh conditions for removing O and reducing the size of the molecules [14]. At least, Ultra Low Sulfur Diesel conditions (i.e. reaction temperature above 350 °C and H_2 pressure above 6 MPa) are required in HDS co-processing of FP or HTL liquids to deoxygenate phenol type compounds. The feasibility to co-process HTL biocrude with VGO by hydroconversion, i.e. operating conditions close to Ultra Low Sulfur Diesel ones, was assessed by Xing et al. [15]. Up to 15 wt% of biocrude

* Corresponding authors.
E-mail addresses: christophe.geantet@ircelyon.univ-lyon1.fr (C. Geantet), yves.schuurman@ircelyon.univ-lyon1.fr (Y. Schuurman).

https://doi.org/10.1016/j.apcatb.2021.120911
Received 16 September 2021; Received in revised form 3 November 2021; Accepted 6 November 2021
Available online 20 November 2021

impacts HDS and HDN (Hydrodenitrofication) performances, but can be a suitable process for upgrading biocrudes [15].

Hydrocracking combines the hydrogenation function of hydrotreating catalysts (NiMo or NiW sulfides on alumina) and an acidic function and requires pressures in the range of 8–20 MPa and temperatures between 300 °C and 450 °C. Hydrodesulfurization aims at reducing the sulfur content to the ppm level. In hydrocracking there is no such objective and thus a possible detrimental competition between deoxygenation, denitrification and desulfurization will have a negligible on the overall performance as the produced middle distillates will be further processed after blending with other feedstocks. Hydrocracking applied to pyrolytic liquids [16] or fractions of pyrolytic liquids [17] was found to produce good quality fuels.

More conventional types of bio-feeds, such as vegetable oils [18], waste cooking oils [19], or waste lubricating oils [20,21] have been investigated in co-hydrocracking with VGO. Co-processing of the FP or HTL liquids mixed with VGO in hydrocracking, has been considered in a limited number of studies, in a two-stage process hydrotreating followed by hydrocracking with a VGO containing 7.5 vol% HTL crude [2] and in a slurry process with a FP liquid up to 20 wt% [22]. One of the difficulties reported in the co-processing of the latter HTL bio-crude is its incompatibility with fossil fuel due to the presence of nonaromatic oxygenates. The lack of compatibility was also explained by the change in the polarity affecting the physicochemical properties [23]. This issue, affecting the reactivity in co-processing of HTL, was studied through fractional distillation to evaluate the different HTL fractions in the co-processing. Oxygen content was mostly detected in the gasoline and jet-fuel fraction of the bio-crude and Hoffmann and al. [24] concluded that hydroprocessing of the bio-crude to remove the oxygenates was needed before the co-processing in existing petroleum refineries.

This work is further exploring and comparing the co-processing of such liquids. More specifically, pretreated 'stabilized' FP liquids and HTL bio-crude were co-fed with VGO at conventional hydrocracking operating conditions and applying a commercial catalyst. The experiments were conducted in a semi-batch reactor, which allowed following the gas production (C_1–C_6 hydrocarbons, CO_2, H_2S) as a function of time. The liquid products were analyzed in detail to evaluate the impact of the bio-liquids on the product composition.

2. Experimental

2.1. Characterization methods

Elemental compositions of feeds and catalyst were analyzed on a Thermo Scientific FLASH 2000 Organic Elemental Analyzer (accuracy of ± 0.1 wt%). Coke content on the used catalyst was determined after washing with heptane to remove any physisorbed hydrocarbons through a solvent extractor after reaction and before analysis.

Simulated distillation analysis was performed on a HP 6890 gas chromatograph (GC) equipped with a flame ionization detector (FID) and a 10 m × 0.53 mm × 0.88 μm ZB-1XT capillary column to analyze the liquid products (mainly naphtha, middle distillates and non-converted feedstock). The relationship between boiling point and retention time for paraffins C6 to C44 was obtained.

NMR data were obtained with a Bruker Avance (250 MHz (^{1}H) 75 MHz (^{13}C)) 5 mm (Quad Nucleus Probe). Inverse gated decoupling and gated spin echo experiments were used to determine hydrocarbons group distribution according to the methods proposed by Cookson et al. [25] and completed by Bouquet et al. [26]. The sample was dissolved in deuterated chloroform. The addition of a paramagnetic relaxation agent such as iron triacetylacetonate was necessary to accelerate the relaxation and ensure a homogeneous relaxation of the different types of carbons. Then, the sample was analyzed by the NMR spectrometer according to 6 different methods: CSE (1/2 J with $J = 125$ Hz (8 ms)) – GASPE (1/2 J with $J = 125$ Hz (8 ms)) – GASPE (1/J with $J = 125$ Hz (4 ms)) – CSE (1/2 J with $J = 160$ Hz (3125 ms)) – GASPE (1/2 J with $J = 160$ Hz (3125 ms)). The processing of the spectra was carried out by Bruker TOPSPIN software. For each spectrum, phasing and baseline correction was performed.

Integration of specific peaks was translated into percentage of a particular type of carbon compared to the total carbons amount. Various carbon types were estimated. Aromatic carbons (C_{ar}) were determined in the 110–160 ppm area in which we were able to estimate quaternary carbons and aromatic CH. Aliphatic carbons (C_{sat}) were estimated from the integration of the 0–65 ppm area of the spectra in which we were able to quantify saturated CH, CH_2, CH_3, paraffinic carbons C_p and naphthenic carbons C_n.

Comprehensive GC×GC-FID and GC×GC-VUV analysis were performed with the Agilent 7890A gas chromatograph equipped with a G3486A CFT differential flow modulator. This system was developed for the analysis of heavy complex feeds (up to C_{60}) [27]. It traces the evolution of families of compounds such as saturated, monoaromatic and polyaromatic species. GC × GC-FID analysis was used for quantitative estimations, while GC × GC-VUV was employed for deciding on areas where product families elute. A VUV detector (VGA-101, VUV Analytics, Inc., Austin, TX, United States, wavelength range 120–430 nm) detector was employed to take benefit of the spectral filtering capabilities of this new type of analyzer [28]. A VUV chromatogram for one of the conversion products is shown in Figs. S1 and S2. Such chromatogram was generated by employing the average absorbance in the 125–240 nm region. Choosing other wavelength regions can offer sensitivity for specific hydrocarbon families. For example, subtracting the average absorbance in 170–205 nm wavelength region from 125 to 240 nm region, allows to highlight the species that absorb in 125–165 nm range and not in 170–205 nm, which corresponds to saturated species (Fig. S2A). Monoaromatics will absorb in 170–205 nm but not in the 205–240 nm region, hence subtracting the average absorbance in the two regions will highlight selectively this hydrocarbon group (Fig. S2B). In such a way information was obtained to generate a GC×GC-FID template. The final template, applied to a GC × GC-FID chromatogram of liquid hydrocracking products, is illustrated in Fig. S3, showing the regions for saturates, monoaromatics and olefins and polyaromatics. A *n*-paraffin mixture, spanning the entire elution temperature range of the sample, was analyzed with the same GC×GC-FID method. In this way, the *n*-paraffin mixture was employed as a reference to generate elution profiles (~ T) for the investigated hydrocarbon families.

Chromatograms were recorded with the following set up: ZB-5HT 1D column (15 m, 0.1 mm ID, 0.1 μm; Phenomenex Co.) and a ZB-35HT 2D column (5 m, 0.25 mm ID, 0.18 μm; Phenomenex Co.). Hydrogen was used as the carrier gas. All samples were diluted in tetrahydrofuran before GC × GC analysis. For all samples, 1 μL injections with a split ratio of 60:1. Details are given by Lelevic et al. [29].

A standard mixture of *n*-paraffins (*n*-C8, *n*-C10, *n*-C12, *n*-C14, *n*-C16, *n*-C20, *n*-C22, *n*-C24, *n*-C26, *n*-C28, *n*-C30, *n*-C32, *n*-C34, *n*-C36, *n*-C38, *n*-C41, *n*-C44, *n*-C50) diluted in carbon disulfide was used for optimization and quantitative performance tests, but also for the generation of the elution profile generation according to boiling point temperature. All chemicals were purchased from Sigma-Aldrich Corporation and were of 99% or greater purity.

GC × GC-MS was performed with a 6890N gas chromatograph (Agilent) equipped with a two-stage thermal modulator (Zoex Corporation, Houston, TX). MS detection was performed with Agilent 5975B Inert MSD quadrupole mass spectrometer.

Reverse column configuration was used with: VF-1701 ms (30 m, 0.5 mm ID, 0.25 μm; Agilent Tech.) in the first dimension and a DB-1 column (3 m, 0.1 mm ID, 0.1 μm; Agilent Tech.) in the second dimension. Carrier gas was helium (99.999% purity). For all samples, 1 μL injections with a split ratio of 100:1 were performed on a 7683 B Agilent split/splitless automatic injector.

ANTEK 9000 nitrogen/sulfur analyzer was used to estimate the sulfur and nitrogen content of liquid products.

Table 1
Properties of VGO.

Elemental analysis (wt%)		Boiling point ranges (wt%)	
C	88.1	Naphta (150 °C)	0.3
H	11.7	Middle distillates (150–360 °C)	9.1
N	0.1	Residue 360 °C+	90.6
O	< 0.2		
H/C atomic ratio (mol/mol)	1.6	**Density (kg/L)**	0.89

Table 2
Elemental analysis of hydrocracking feedstock.

Bio-liquid	C (wt%)	H (wt%)	N (wt%)	O (wt%)	S (wt%)	H/C
SPO	52.6	9.1	0.5	37.0	< 0.1	2.1
SDPO	85.5	12.2	0.2	2.3	< 0.1	1.7
HTL	80.0	12.2	1.1	10.2	n.d.	1.8

2.2. Feedstock properties

The VGO crude oil feed taken was a mixture of 74 wt% mildly hydrotreated vacuum gas oil and 26 wt% decanted recycle oil, provided by REPSOL (Table 1). Three bio-liquids with different oxygen contents were used in this study: two were issued from fast pyrolysis units and one from a hydrothermal liquefaction (HTL) unit (Table 2). The fast pyrolysis liquids, SDPO (stabilized deoxygenated pyrolysis oil) and SPO (stabilized pyrolysis oil) were provided by BTG (Biomass Technology Group BV). These bio-liquids were obtained by fast pyrolysis of pine wood previously described [3]. For FP bio-liquids, pretreatment processes were carried out before these co-processing tests [30];

- SPO is obtained from fast pyrolysis oil that has been partially hydrogenated to stabilize the most reactive oxygen moieties. This "stabilization" step, carried out between 175 and 250 °C over a Ni-based catalyst (Picula™), transforms mainly the sugars into polyalcohols [31,32]. SPO is more stable than pyrolysis oil, has less tendency for polymerization and is less acid. This stabilization steps consume low amounts of hydrogen (only 20% of the total amount needed for full deoxygenation) and SPO still has a high oxygen content. This makes them especially suited for further processing, as already shown for co-processing in FCC units [3].
- The SDPO has been, after stabilization, deoxygenated to further reduce the oxygen level to obtain a C/H ratio closer to that of petroleum feeds. This was accomplished by treating the stabilized bio-liquid (SPO), after water removal, over a sulfide supported CoMo catalyst at 350 °C at 200 bar of hydrogen pressure. SDPO is not the best choice for hydrocracking as it has been almost completely hydrodeoxygenated, but is used in this study to evaluate the impact of the pyrolysis molecules other than the oxygenated components.

The HTL bio-crude, provided by Aalborg University in Denmark, was produced through hydrothermal liquefaction of pine wood and its oxygen content lies between that of SDPO and SPO. This bio-crude is quite stable for processing and storage and does not need any additional stabilization.

The Van Krevelen diagram plot shows the atomic H/C and O/C ratio of each feedstock based on the elemental analysis data in Fig. S4 of Supplementary information (S.I.). The untreated pyrolysis liquid is also shown in Fig. S4, demonstrating that the "stabilization" to yield SPO hardly affects the O/C ratio, but rather increases the H/C ratio (as expected for the conversion of sugars into polyalcohols). Further hydrogenation of SPO into SDPO decreases strongly the O/C ratio, with little impact on the H/C ratio. The GCxGC-MS chromatograms of bio-liquids are presented in the S.I. (Figs. S5, S6 and S7). Chemical composition of the bio-liquids determined by ^{31}P NMR are also presented (Fig. S8) showing that HTL and SDPO contain mostly ArOH groups, whereas, in SPO bio-liquid, ROH are the predominant groups.

Table 3
Hydrocracking product families according to boiling point range.

Family	Temperature
Gas	< 35 °C
Naphtha	35–150 °C
Kerosene	150–250 °C
Diesel	250–360 °C
Middle distillates	150–360 °C
Bottom	> 360 °C

2.3. Catalyst

The catalyst extrudates used for this study was a proprietary sulfided NiMo containing Y-zeolite (Axens). The catalyst sulfidation was done with a 4 L/h flow (3.6 L/h of H_2 and 0.4 L/h of H_2S) for 4 h at 400 °C with a 5 °C/min ramp rate before reaction.

2.4. Hydrocracking experiments

Hydrocracking experiments were performed in a 250 cm^3 semi-batch stirred-tank reactor, with a 6-blade gas-inducing impeller and an H_2 inlet distributor. A condenser and a cold separator were included in the system to recover the gas and condensables. The gas outlet flow was measured with good repeatability and high precision by a Brooks instrument Quantim Series Coriolis Flow Meter and analyzed on-line by a micro-GC (SRA Instrument R3000 series) containing two modules PoraPLOTU (8 m × 0.32 mm ID) and OV1 (8 m × 0.15 mm ID). A detailed description of the equipment is given elsewhere [33]. The on-line analysis allowed quantification of C1-C6 hydrocarbons, H_2, H_2S and CO_2, but not, NH_3 (dissolved in water), CO and H_2O. Water was (partly) quantified after reaction in the liquid fraction collected in the condenser by Karl-Fischer titration, but a small amount condensed in the top part of the batch reactor.

Hydrocracking experiments were performed at 380 °C or 400 °C for 5 h. In each experiment 110 g of charge (VGO pure or blend with HTL, SDPO or SPO) were mixed with 10 g of sulfided catalyst and 0.3 g of propylamine in the reactor. Propylamine was used to temper the acidity of the zeolite to avoid excessive cracking toward light products, as shown in previous studies highlighting that a milder acid strength will promote a more selective cracking toward middle distillates [34]. At the start of each experiment the reactor was pressurized with 120 bars of hydrogen and then heated to the desired reaction temperature.

Conversion of products with boiling points above 360 °C and middle distillates (MD) selectivity were determined by the following formulas:

$$Conversion = \frac{\text{mass } 360\ ^\circ\text{C}^+_{t=0} - \text{mass } 360\ ^\circ\text{C}^+_t}{\text{mass } 360\ ^\circ\text{C}^+_{t=0}}$$

$$Selectivity\ MD = \frac{\text{mass MD}}{\text{mass } 360\ ^\circ\text{C}^+_{t=0} - \text{mass } 360\ ^\circ\text{C}^+_t}$$

The VGO contains 90.6 wt% 360 °C+ (Table 1). This was taken into account to calculate the conversion. Experimental mass balances were between 88 and 99 wt%. Mass losses were associated to the difficult recovery of liquid product from the catalyst and the reactor. Replicate experiments showed that the product distribution did not depend on the recovery content.

Hydrocracking products were classified into families according to their boiling point range listed in Table 3.

3. Results

GC × GC-MS analyses of the pure bio-liquids provided insight into

Table 4
Conversion ($X_{360\,°C+}$) and middle distillates selectivity (S_{MD}) of hydrocracking experiments.

Feed	T (°C)	$X_{360\,°C+}$ (%)	S_{MD} (%)
VGO	380	52.6 (55.7)[a]	60.0 (62.7)[a]
VGO	400	79.9	30.3
VGO + SDPO (10%)	380	58.3	52.1
VGO + SPO (10%)	380	54.1	61.1
VGO + SPO (20%)	380	50.8	52.1
VGO + SPO (10%)	400	84.9	27.5
VGO + HTL (10%)	380	40.9 (41.0)[a]	69.8 (70.5)[a]
VGO + HTL (20%)	380	38.8	67.3
VGO + HTL (10%)	400	71.7	43.0

[a] Repeated experiment.

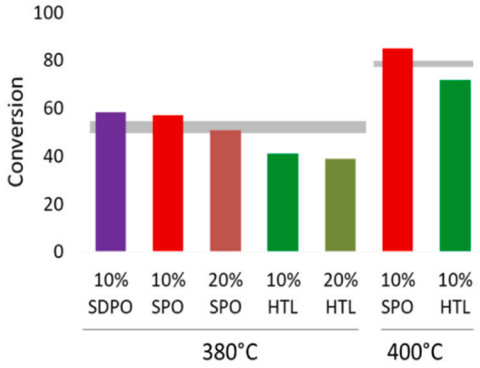

Fig. 1. VGO conversion for co-processing of bio-liquids. The grey horizontal bars indicate the VGO conversion for VGO hydrocracking only at the corresponding temperature (The width of this bar is proportional to the experimental error).

their chemical composition. The GC × GC chromatograms are summarized in the S.I. (Figs. S5–S7). While SPO contains mostly oxygenated species (phenol, methoxy etc.), HTL is characterized by a significant content of paraffins, monoaromatics and polyaromatics among which phenanthrene species are dominant. Both bio-liquids were also analyzed by GC × GC-FID, which was used to derive the quantity of the most abundant peaks. The quantity of phenanthrene species in HTL was approximately 7 wt%, while the most abundant methoxy species in SPO accounted for approximately 6 wt%.

Table 4 summarizes the hydrocracking experiments performed in terms of 360 °C+ conversion and middle distillates selectivity, the main product of hydrocracking. The boiling point curves from simulated distillation results are given in Table S1 in the S.I. Co-processing with HTL and SPO were performed in two mass ratios of VGO/bio-liquid (90/10 and 80/20 wt%). Reactions were performed at 380 °C and at 400 °C. The hydrogen consumption in a typical semi-batch experiment was estimated in between 6 and 7 g for 110 g of feedstock, which is slightly higher than reported in other studies [35]. The hydrogen consumption did not show any trend with the nature of the feed, probably due to the too low accuracy of the measurements.

Hydrocracking constitutes many reactions occurring in parallel and series. While the product selectivities depend therefore strongly on the conversion level, to correctly interpret the impact of the bio-liquid on the hydrocracking the selectivities of the different experiments the selectivity and product compositions are compared at similar conversion levels. We have conducted the co-processing experiments at the same conditions as the VGO hydrocracking, but the addition of the bio-liquid sometimes changes the 360 °C+ conversion. In this section we analyze the data as a function of the 360 °C+ conversion to understand the general trends to conclude the impact of the bio-liquids. More analyzes have been carried out and are reported in the SI, but not all data are at

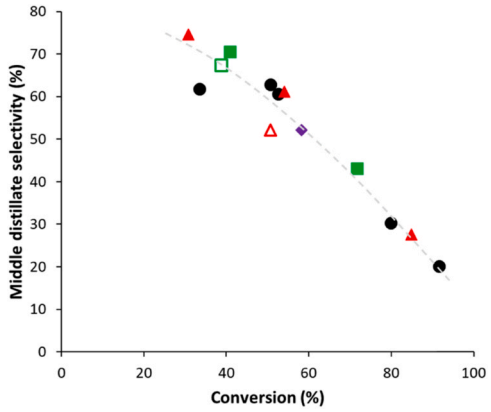

Fig. 2. Selectivity of middle distillate versus 360 °C+ conversion. •: VGO, ◆: VGO + 10% SDPO, ■: VGO + 10% HTL, □: VGO + 20% HTL, ▲: VGO + 10% SPO, △: VGO + 20% SPO.

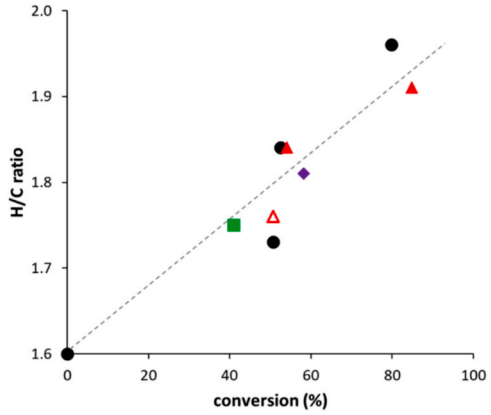

Fig. 3. H/C ratio versus 360 °C+ conversion. •: VGO, ◆: VGO + 10% SDPO, ■: VGO + 10% HTL, ▲: VGO + 10% SPO, △: VGO + 20% SPO.

iso-conversion level. Fig. 1 shows that the nature and quantity of the bio-liquid has an effect on the 360 °C+ conversion compared to VGO hydrocracking.

Co-processing SDPO/SPO resulted in similar or slightly higher conversion levels compared to VGO hydrocracking, but co-processing HTL led to a significant lower activity. Fig. 2 illustrates the general trend in hydrocracking with the decrease in selectivity when conversion increases due to consecutive cracking of the middle distillate fraction into naphtha and gas, in agreement with other studies [36]. This tendency was independent of the reaction conditions or the feedstock nature.

Not only cracking reactions occur but also hydrogenation reactions take place. This can be seen by the linear increase of the H/C ratio with increasing conversion (Fig. 3). Detailed characterization of gas, liquid and solid products are given hereafter.

3.1. Gas phase analysis

The gas production could be followed on-line. Fig. 4 shows gas yields for hydrocracking experiments at 380 °C and 120 bars H_2 with VGO and VGO/SPO 90/10 wt%, VGO/HTL 90/10 wt% blends.

The starting time corresponds to the beginning of the pressurization phase, which took place before the heating phase. It took approximately

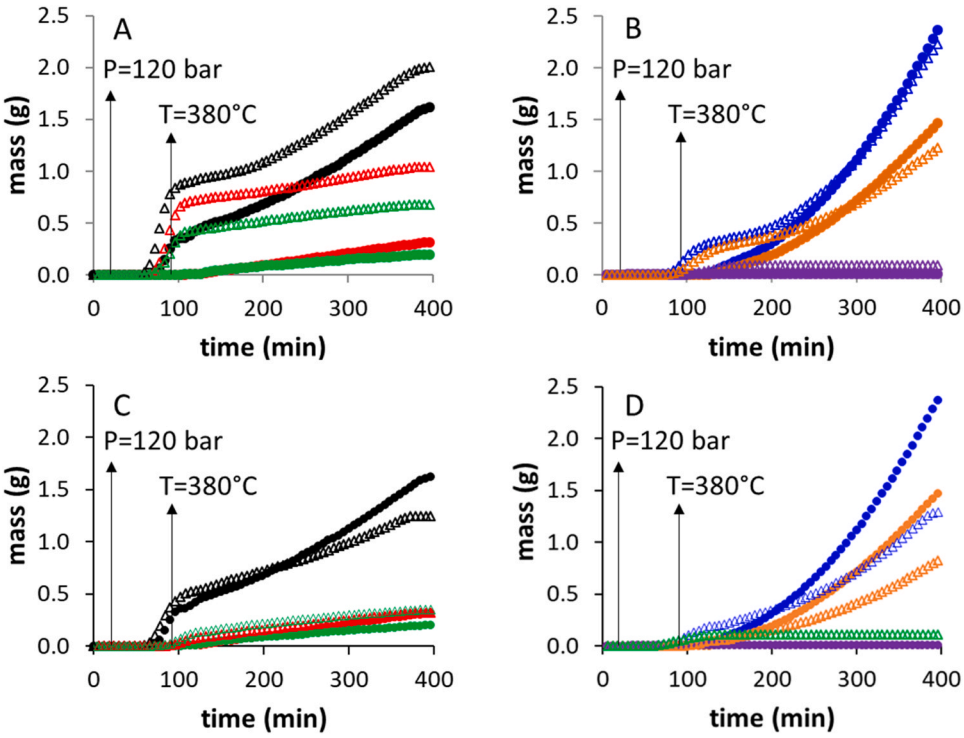

Fig. 4. Cumulative plots for gas phase analysis of light hydrocarbons for hydrocracking at 380 °C and 120 bars H_2. **A**: C1 VGO (•), C1 VGO/10% SPO (Δ), C2 VGO (●), C2 VGO/10% SPO (△), C3 VGO (●), C3 VGO/10% SPO (△). **B**: C4 VGO (●), C4 VGO/10% SPO (△), C5 VGO (●), C5 VGO/10% SPO (△), C6 VGO (●), C6 VGO/10% SPO (△). **C**: C1 VGO (•), C1 VGO/10% HTL (Δ), C2 VGO (●), C2 VGO/10%HTL (△), C3 VGO (●), C3 VGO/10% HTL (△). **D**: C4 VGO (●), C4 VGO/10% HTL (△), C5 VGO (●), C5 VGO/10% HTL (△), C6 VGO (●), C6 VGO/10% HTL (△).

75 min to heat up the reactor to 380 °C. The gas production for the hydrocracking of pure VGO typically started once the temperature had reached 380 °C, except for C_3 products that were formed already at lower temperatures. For co-processing experiments with both SPO and HTL, light hydrocarbons C1–C3 were produced before the temperature reached 380 °C. The C1–C3 fractions increased very rapidly initially and then slowed down, showing a similar increase as the pure VGO experiments. Bergvall et al. reported a similar observation [22].

Fig. 5 shows the CO_2 production for VGO, VGO/SPO and VGO/HTL hydrocracking experiments at 380 °C. Decarboxylation reactions started well before the final reaction temperature was reached, and only lasted for a short period of time. These reactions, leading to the formation of CO_2, were more pronounced for the VGO/SPO rather than for the VGO/HTL blends. The rates for decarboxylation (derivative of the CO_2 concentration with respect to time) were quite similar for the two blends of bio-liquids.

Fig. 6 shows the evolution of H_2S. H_2S production started during the heating-up phase of the reactor and then increased continuously with time, but with a lower rate. This might indicate a continuous desulfurization reaction for the various sulfur compounds in a wide range of reactivities.

3.2. Liquid phase analysis

A simulated distillation of the liquid product fraction compared with the total elution profile determined by GCxGC-FID is represented in Fig. S9. The two profiles overlap completely, validating the technique. The GC×GC-FID method, along with the generated template has allowed generating elution profiles for three hydrocarbon families of interest: polyaromatics, monoaromatics and saturated hydrocarbons (Fig. 7). The composition of the various feeds is shown at zero conversion. A linear decrease of both the monoaromatic and polyaromatics with increasing conversion was observed, although the polyaromatics decreased much faster. At the same time the saturated hydrocarbons increased. Hydrogenation of the polyaromatics led to monoaromatics, while both could give cycloalkanes and alkenes and ring opening could lead to saturated hydrocarbons.

3.2.1. ^{13}C NMR analysis

High-resolution ^{13}C NMR characterization was conducted to gain better understanding of the composition of the liquid products. The

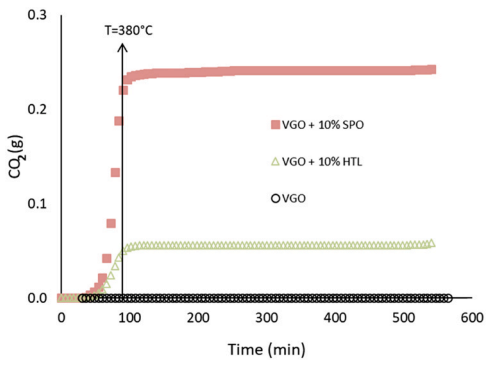

Fig. 5. Cumulative CO_2 analysis for hydrocracking at 380 °C and 120 bars H_2 for 5 h. ○ VGO, ■ VGO/10% SPO, △ VGO/10% HTL.

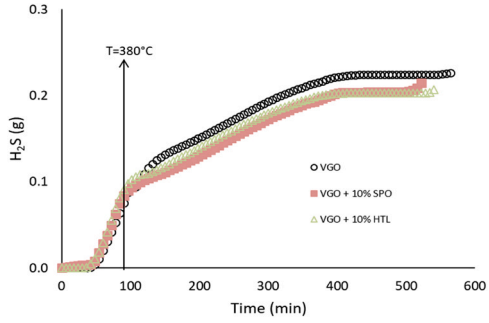

Fig. 6. Cumulative H_2S analysis for hydrocracking at 380 °C and 120 bars H_2 for 5 h. ○ VGO, ■ VGO/10% SPO, △ VGO/10% HTL.

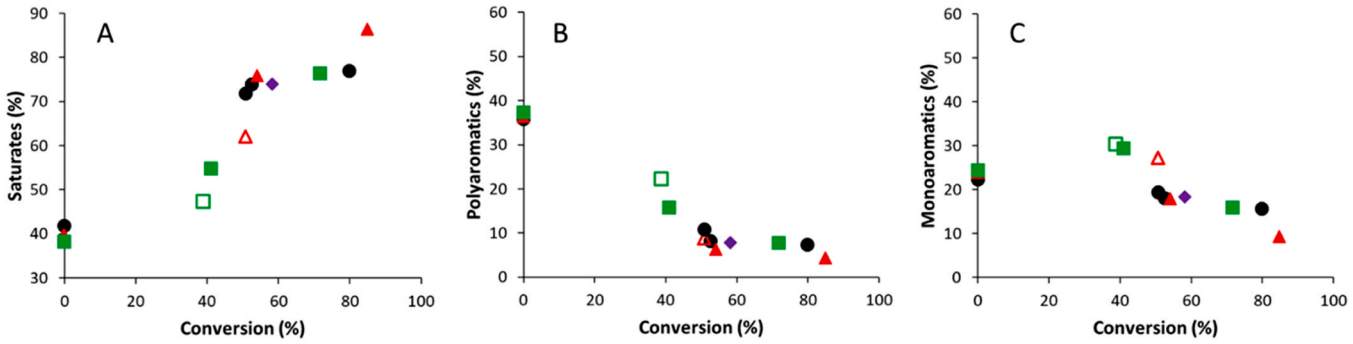

Fig. 7. Monoaromatics, polyaromatics and saturated hydrocarbons evolution obtained by GCxGC versus 360 °C+ conversion. •: VGO, ◆: VGO + 10% SDPO, ■: VGO + 10% HTL, □: VGO + 20% HTL, ▲: VGO + 10% SPO, △: VGO + 20% SPO.

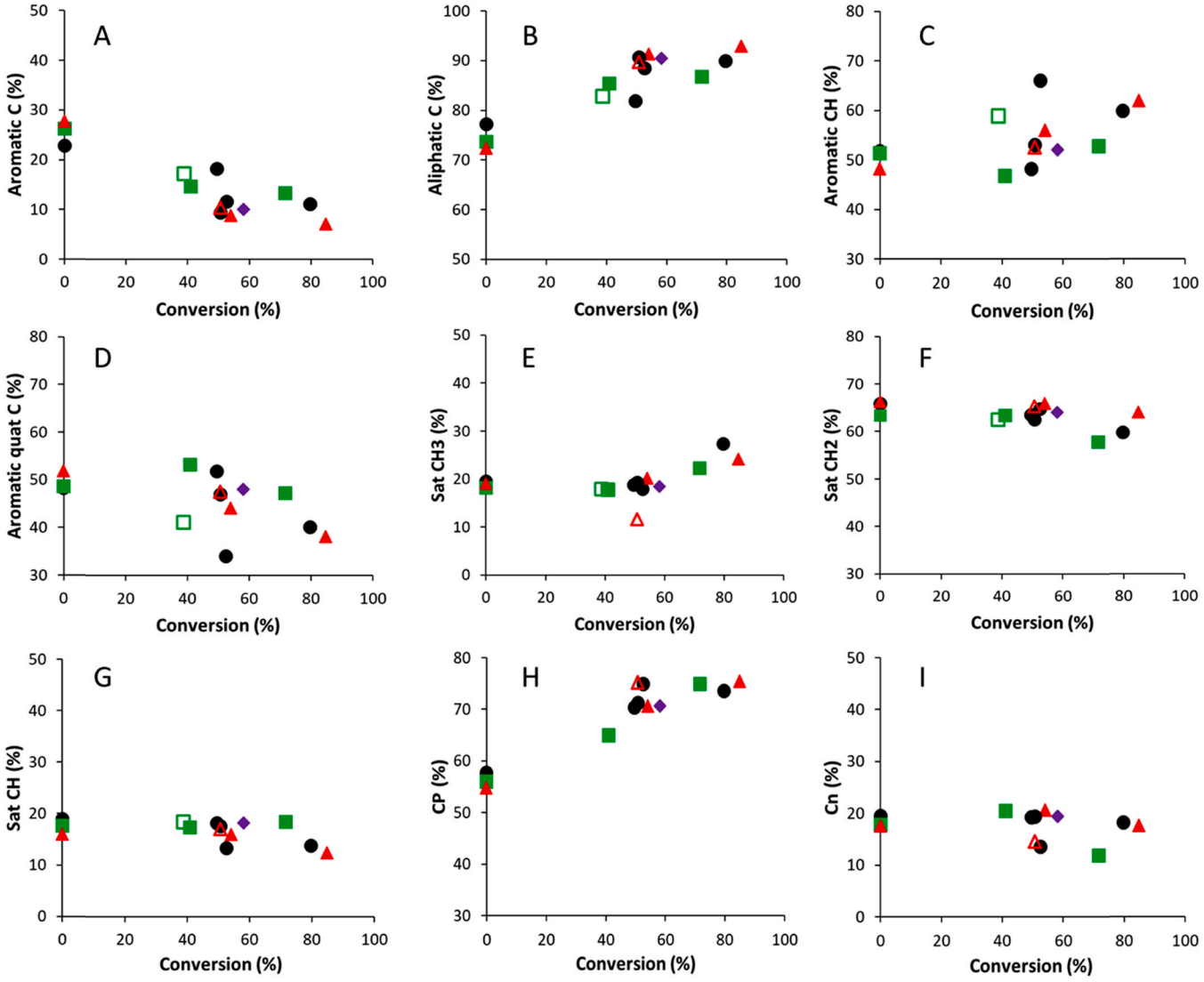

Fig. 8. Evolution of the carbon repartition (aromatic C, aliphatic C, aromatic CH, aromatic quaternary C, saturated CH_2, CH_3 and CH, paraffinic C and naphthenic C) obtained by ^{13}C NMR as a function of the 360 °C+ conversion. •: VGO, ◆: VGO + 10% SDPO, ■: VGO + 10% HTL, □: VGO + 20% HTL, ▲: VGO + 10% SPO, △: VGO + 20% SPO.

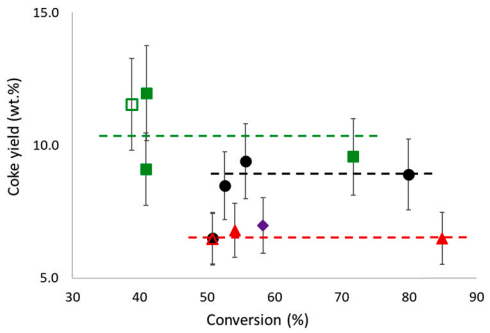

Fig. 9. Coke yield expressed as wt% of catalyst mass for hydrocracking experiments of VGO and VGO + bio-liquid. Symbols: Experimental data; Green dashed line (top): trend for VGO/HTL, Black dashed line (middle): trend for VGO, Red dashed line (bottom): trend for VGO/SPO, SDPO. •: VGO, ◆: VGO + 10% SDPO, ■: VGO + 10% HTL, □: VGO + 20% HTL, ▲: VGO + 10% SPO, △: VGO + 20% SPO.

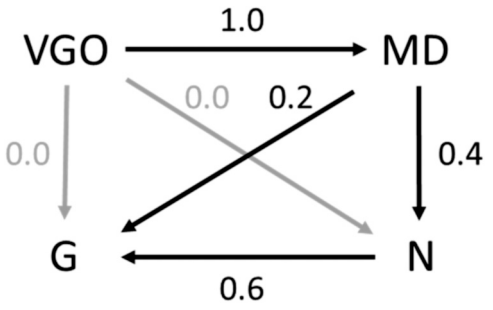

Fig. 10. 4-lump model for hydrocracking with VGO as feed, middle distillates (MD), naphtha (N) and gas (G) as products. The numbers close to the arrows are the values of the normalized rate constants.

method used based on Cookson et al. procedure [25] aimed at quantify different types of carbons, and thus obtain information of multiplicity.

Various carbon types were estimated aromatic, saturated, paraffinic and naphthenic carbons (C_{ar}, C_{sat}, C_p, C_n). The evolution of each carbon type as a function of the 360 °C+ conversion is illustrated in Fig. 8. The composition of the various feeds is shown at zero conversion. A decrease of aromatics and an increase of aliphatic carbons as a function of the 360 °C+ conversion was observed, in agreement with the GCxGC results. A decrease of aromatic quaternary carbon could be noticed, which was partly transformed into aromatic CH increasing with increasing conversion. At the same time a decrease of the saturated CH_2 and CH is observed, part of which was probably transformed into saturated CH_3 increasing with increasing conversion. Naphthenic carbons (C_n) slightly decreased when the conversion increased, showing that during the hydrocracking reactions, a fraction of the naphthenic carbons was converted into paraffinic carbons (C_p).

To estimate HDS and HDN performances, the amount of sulfur and nitrogen in the feedstock and liquid products was measured. Sulfur and nitrogen in the VGO feedstock were estimated at approximately 1168 ppm and 1043 ppm, respectively. After reaction, the amount of sulfur and nitrogen were less than 50 ppm, which was below the detection limit. Thus, HDS and HDN conversions are well above 95%.

3.3. Solid phase analysis

CHNS analyses of the spent catalysts were performed to assess the coke amount produced during the reaction. Fig. 9 shows the amount of carbon determined on the catalyst after reaction. The complete data set might have suggested a slightly decreasing trend with increasing 360 °C+ conversion, but the data separated for each blend showed a rather constant level, with the addition of HTL producing more coke and the addition of SPO producing less coke than pure VGO hydrocracking.

On average the catalyst sulfur content dropped from 7 wt% for a freshly sulfide sample to 5.5 wt% after reaction.

4. Discussion

Hydrocracking takes place over a bifunctional catalyst, consisting of a metal-sulfide phase and an acidic function. Hydrogenation / dehydrogenation equilibrium is established over the metal-sulfide phase, yielding low concentrations of olefins. These olefins migrate and are protonated inside the zeolite forming carbenium ions. The carbenium ions undergo a series of reactions: isomerization by hydride or methyl shifts or by PCP (protonated cyclopropane) branching, β-scission, dealkylation of aromatics and cyclization [37–39].

For sulfided catalysts, such as the one used in this study, desulfurization and denitrification reactions also take place, producing H_2S and NH_3, respectively. Due to large number of different molecules present in the initial VGO and the large number of possible reactions, modeling of hydrocracking has been a challenging task. While detailed models such as a model based on 217 pseudo-components [40] or continuous lumping model [41] are available, most of models are based on lumps (4 lumps models) representing product fractions according to their boiling point range have been used initially [42–44]. To quantify the impact of the bio-liquids on the VGO hydrocracking and allow interpolation of the selectivity and yields as a function of the conversion, we also propose a 4-lumped model, as shown in Fig. 10. It shows the VGO/bio-liquid conversion into middle distillates, naphtha and gas together with the corresponding normalized rate constants. The rate constants were estimated by regression analysis of all the experimental data simultaneously. This choice was motivated by the fact that the middle distillate selectivity as a function of the conversion did not show any systematic deviations for all the blends (Fig. 2). Note that for these calculations the mass balances have been normalized to 100%, resulting in a slightly different conversion. VGO/bio-liquid is consecutively cracked into middle distillates and naphtha, while both middle distillates and naphtha further crack to gas. The rates of naphtha and gas production from VGO were estimated to be negligible. This implies that MD is the primary product of the hydrocracking and that the MD selectivity decreases continuously with increasing conversion, as can be seen for the experimental data in Fig. 2. Fig. 11 compares the model fit with the experimental data. The different symbols represent the different co-processing experiments. Scattering of the data around the model predicted yields (full lines) for middle distillates and naphtha are similar for all experiments; i.e. independent of the nature and quantity of the co-processed feed. Thus, the middle distillates and naphtha selectivities are not significantly impacted by addition of either pyrolysis oil or HTL biocrude. Alvarez-Majmutov et al. [45] reached a similar conclusion with respect to the yields of the naphtha and diesel fractions by co-processing deoxygenated pyrolysis oil with VGO through hydrocracking.

However, the gas profiles in Fig. 4 clearly showed a fast production of the C1-C5 hydrocarbons for the co-processing experiments that started slightly before the reaction temperature had been reached. This fast production is absent for pure VGO hydrocracking. After this fast rise, the slope of the subsequent gas production in the presence of bio-liquid was similar to that of pure VGO hydrocracking. This initial gas production was more pronounced for the C1–C3 fractions than for C4–C5, and was almost negligible for the C6 fraction. It was also more pronounced for SPO than HTL co-processing. The CO_2 evolution depicted in Fig. 5, also showed initially a fast production that then drops to zero. The CO_2 yield did not depend on the VGO conversion, only on the type and quantity of bio-liquid introduced, as did the approximate water production, illustrated in Fig. S10. SPO yielded more CO_2 and H_2O than HTL as it has a higher initial oxygen content. These trends indicate that before reaching the hydrocracking reaction temperature, decarboxylation (and very

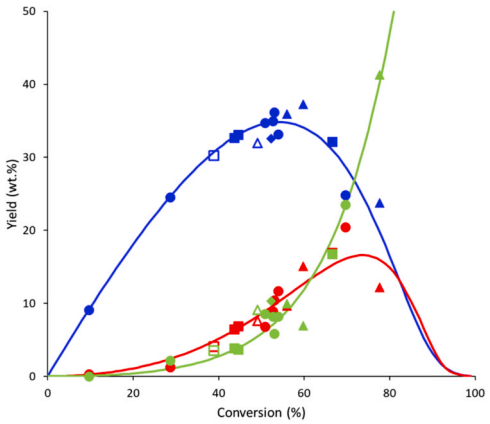

Fig. 11. Product distribution of middle distillates (blue), naphtha (red) and gas (green). Symbols: Experimental data; Lines: 4-lump model fit. •: VGO, ◆: VGO + SDPO, ■: VGO + HTL, ▲: VGO + SPO. Full symbols 10 wt% bio-liquid blend, open symbols 20 wt% bio-liquid blend.

likely decarbonylation, although the CO production could not be followed during the experiments) of the bio-liquid already occurred, accompanied by the production of light hydrocarbons. The hydrocracking, under co-processing conditions, then continued with a (partly) deoxygenated bio-liquid. The overall co-processing can thus be regarded as a two-step sequential process, with HDO followed by hydrocracking. HDO of SPO will yield more CO_2, H_2O and light gases than HDO of HTL as the oxygen content of the former is higher (Table 2). Different studies have shown that decarboxylation, decarbonylation and deoxygenation steps for pyrolysis liquids indeed readily occur at temperatures between 320 and 350 °C over NiMo sulfide catalysts [46,47]. The presence of a petroleum fraction has a positive effect on the HDO reactions, by preventing polymerization and favoring hydrogen transfer [48,49]. Pstrowska et al. reached > 97% deoxygenation during hydrorefining of 20% (v/v) rapeseed pyrolysis bio-oil and 80% (v/v) light gas oil fraction blend at 260 °C [48]. Although the water production could not be followed during the hydrocracking, the cited studies indicate that deoxygenation through the formation of water also occurs at lower temperatures than hydrocracking.

The H_2S production also started at temperatures lower than 380 °C, as shown in Fig. 6, but contrary to the CO_2 production it continued during the whole further hydrocracking experiment. An inflection in the rate of H_2S formation was observed at a level of 0.1 g, which roughly corresponded to the total amount of sulfur in the feed (~ 1100 ppm). The subsequent lower rate of H_2S production suggested the presence of more refractory sulfur-containing compounds. After reaction a few tenth ppm of sulfur was still present in the liquid product, which might be compounds like (di-) naphthodibenzothiophenes [50]. Some of the H_2S originated from desulfurization of the catalysts as the catalyst sulfur content after reaction had decreased.

No impact on the final sulfur content is observed of co-processing FP or HTL bio-liquid, as the H_2S production rates were very similar. The desulfurization started at the same time/temperature as the decarboxylation, suggesting that no competition occurred between the two processes. This is line with the sulfur contents of the liquid products that were below the detection limit for all experiments. This is a different result than in the case of co-hydrotreating, where a strong competition between the oxygenated and sulfur containing molecules results in a reduced desulfurization activity [51].

Figs. 7 and 8 show the detailed composition of the liquid product in terms of aromatics and paraffins. The global trends show that poly-aromatics were cracked into mono-aromatics and that hydrogenation of aromatics into paraffins and cycloalkanes occurred. This is expected for hydrocracking under high hydrogen pressures, proceeding through the above-mentioned reactions. The same trend was observed in the case of co-processing experiments. The observed scattering of the data around the global trend was again independent of the nature and quantity of the co-processed feed. This is consistent with a two-step process of HDO followed by hydrocracking. Alvarez-Majmutov et al. [45] also observed a net aromatics conversion independent of the VGO/bio-oil blend. Thus, the liquid product composition was not impacted by addition of either pyrolysis oil or HTL biocrude.

The catalyst coke content displayed in Fig. 9 can be grouped by different blends and in that case the "coke" formation seems to be independent of the 360 °C+ conversion and decreases as VGO/HTL > VGO > VGO/SPO. The VGO/HTL blend had an impact on the catalyst activity, as lower conversion levels were observed compared to VGO hydrocracking, shown in Fig. 1. This might be due to site blocking by coke deposits on the catalyst as a higher catalyst coke level was observed for the VGO/HTL blend (Fig. 9). The conversion levels for the hydrocracking experiments at 380 °C correlate with the catalyst coke content after reaction (Fig. S11). The coke propensity of the feeds has not been measured, but micro carbon residue test (MCRT) values for similar pyrolysis liquids have been reported [3]. MCRT values for SPO bio-liquids are much higher than for VGO (~ 20 versus 0.6 wt%), while lower catalyst coke content was found for VGO/SPO co-processing than VGO hydrocracking. Alvarez-Majmutov et al. [45] did not observe any accelerated catalyst deactivation in the presence of bio-oil fractions, although these fractions where deoxygenated to higher extent than the ones used here. An alternative explanation for the lower activity when co-processing HTL bio-liquid might be due to the presence of the heavier mass fraction in HTL or a fraction that is more difficult to crack than SPO. This is supported by the similar conversion levels for HTL co-hydrocracking at 380 °C and the increased conversion at 400 °C.

From the model it appears that hydrocracking of VGO/bio-liquid blends occurs via a two-step process, as schematized in the lumped model in Fig. 12. Even before the reaction temperature of 380 °C is reached, hydrodeoxygenation takes place producing CO_x and H_2O. Unfortunately, no oxygen mass balance could be established as CO was not analyzed and especially only fraction of the water was quantitatively recovered after reaction. Only for the VGO + 20 wt% SPO feed, trace amounts of oxygenated components, such as alkyl-methoxy-phenols, were observed in the liquid products by GCxGC analysis. The corresponding GCxGC chromatograms for the HTL (10 & 20 wt%) and SPO (10 & 20 wt%) are given in the SI (Figs. S13–S16). However, as observed from the rate of CO_2 production as a function of time, decarboxylation runs quickly to completion. HDO is facilitated by the metal-sulfide phase, which can activate molecular hydrogen. Although reactions such as decarboxylation and dehydration occur over acid zeolite sites, these reactions take place at much higher temperatures (> 500 °C) [52]. During HDO, light hydrocarbons are produced as well [49]. The deoxygenated bio-liquid resembles a heavy petroleum feed and is therefore readily hydrocracked together with VGO according to the established bi-functional reaction steps. Therefore, the product distribution, except a slightly higher gas production and CO_x, is not impacted by the nature and quantity (up to 20 wt% in this study) of the bio-liquid. The same is true for the composition of the liquid products. The selectivity and product composition mainly depend on the 360 °C+ conversion level, but the conversion depends on the nature of the VGO/bio-liquid blend.

5. Conclusions

Co-processing hydrocracking experiments of VGO with different bio-liquids, stabilized pyrolysis liquid (SPO), stabilized deoxygenated pyrolysis liquid (SDPO) and hydrothermal bio-crude (HTL), were performed in a semi-batch reactor. All data were scattered around a trend of decreasing middle distillate selectivity with increasing conversion. Co-processing SPO resulted in similar conversion then hydrocracking VGO, while co-processing with HTL led to slightly lower conversion. Analysis of the gas phase products as a function of time, revealed that decarboxylation precedes hydrocracking. This reaction takes place at

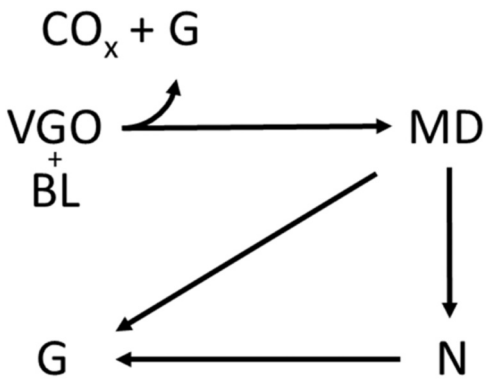

Fig. 12. Lumped model for co-processing SPO and HTL bio-liquids (BL) with VGO through hydrocracking into middle distillates (MD), naphtha (N) and gas (G).

lower reaction temperatures than hydrocracking and is completed before the reactor reaches the final reaction temperature. Therefore, even in the case co-processing bio-liquids, hydrocracking occurs with a largely deoxygenated feed. As a result, the product distribution is hardly affected by blending in bio-liquids. Detailed analysis of the liquid phase composition showed no differences in the mono- and polyaromatics as well paraffins concentrations. Due to the fast "in-situ" hydro-deoxygenation of the bio-liquids, the hydrocracker might well be an appropriate entry point into a refinery for the production of bio-fuels, eliminating a separate hydrodeoxygenation process, although this needs further research as the (pre-)heating of the feed in an industrial hydrocracker is very different than used here.

CRediT authorship contribution statement

Donia Bouzouita: Investigation, Writing – original draft. **Aleksandra Lelevic**: Investigation, Formal analysis. **Chantal Lorentz**: Investigation, Formal analysis. **Robbie Venderbosch**: Resources, Writing – review & editing. **Thomas H. Pedersen**: Resources, Writing – review & editing. **Christophe Geantet**: Writing – review & editing, Supervision. **Yves Schuurman**: Writing – review & editing, Supervision, Funding acquisition.

Declaration of Competing Interest

The authors declare that they have no known competing financial interests or personal relationships that could have appeared to influence the work reported in this paper.

Acknowledgments

This project has received funding from the European Union's Horizon 2020 Research and Innovation Programme ("4REFINERY") Grant agreement no. 727531.

Appendix A. Supplementary material

Supplementary data associated with this article can be found in the online version at doi:10.1016/j.apcatb.2021.120911.

References

[1] P.L. Cruz, D. Iribarren, J. Dufour, Life cycle costing and eco-efficiency assessment of fuel production by coprocessing biomass in crude oil refineries, Energies 12 (24) (2019) 4664, https://doi.org/10.3390/en12244664.
[2] S. Badoga, A. Alvarez-Majmutov, T. Xing, R. Gieleciak, J. Chen, Co-processing of hydrothermal liquefaction biocrude with vacuum gas oil through hydrotreating and hydrocracking to produce low-carbon fuels, Energy Fuels 34 (6) (2020) 7160–7169, https://doi.org/10.1021/acs.energyfuels.0c00937.
[3] L. Gueudré, F. Chapon, C. Mirodatos, Y. Schuurman, R. Venderbosch, E. Jordan, S. Wellach, R.M. Gutierrez, Optimizing the bio-gasoline quantity and quality in fluid catalytic cracking co-refining, Fuel 192 (2017) 60–70, https://doi.org/10.1016/j.fuel.2016.12.021.
[4] S. Bezergianni, A. Dimitriadis, O. Kikhtyanin, D. Kubička, Refinery co-processing of renewable feeds, Prog. Energy Combust. Sci. 68 (2018) 29–64, https://doi.org/10.1016/j.pecs.2018.04.002.
[5] G. Fogassy, N. Thegarid, G. Toussaint, A.C. van Veen, Y. Schuurman, C. Mirodatos, Biomass derived feedstock co-processing with vacuum gas oil for second-generation fuel production in FCC units, Appl. Catal. B: Environ. 96 (3) (2010) 476–485, https://doi.org/10.1016/j.apcatb.2010.03.008.
[6] A. de Rezende Pinho, M.B.B. de Almeida, F.L. Mendes, V.L. Ximenes, L. C. Casavechia, Co-processing raw bio-oil and gasoil in an FCC unit, Fuel Process. Technol. 131 (2015) 159–166.
[7] Y. Mathieu, L. Sauvanaud, L. Humphreys, W. Rowlands, T. Maschmeyer, A. Corma, Opportunities in upgrading biomass crudes, Faraday Discuss. 197 (2017) 389–401, https://doi.org/10.1039/C6FD00208K.
[8] J. Scherzer, A.J. Gruia, Hydrocracking Science and Technology, CRC Press, 1996.
[9] J.W. Ward, Hydrocracking processes and catalysts, Fuel Process. Technol. 35 (1) (1993) 55–85, https://doi.org/10.1016/0378-3820(93)90085-I.
[10] G. Valavarasu, M. Bhaskar, K.S. Balaraman, Mild hydrocracking—a review of the process, catalysts, reactions, kinetics, and advantages, Pet. Sci. Technol. 21 (7–8) (2003) 1185–1205, https://doi.org/10.1081/LFT-120017883.
[11] S. Mohanty, D. Kunzru, D.N. Saraf, Hydrocracking: a review, Fuel 69 (12) (1990) 1467–1473, https://doi.org/10.1016/0016-2361(90)90192-S.
[12] R. Sahu, B.J. Song, J.S. Im, Y.-P. Jeon, C.W. Lee, A review of recent advances in catalytic hydrocracking of heavy residues, J. Ind. Eng. Chem. 27 (2015) 12–24, https://doi.org/10.1016/j.jiec.2015.01.011.
[13] J. Martínez, J.L. Sánchez, J. Ancheyta, R.S. Ruiz, A review of process aspects and modeling of ebullated bed reactors for hydrocracking of heavy oils, Catal. Rev. 52 (1) (2010) 60–105, https://doi.org/10.1080/01614940903238858.
[14] P. Grange, E. Laurent, R. Maggi, A. Centeno, B. Delmon, Hydrotreatment of pyrolysis oils from biomass: reactivity of the various categories of oxygenated compounds and preliminary techno-economical study, Catal. Today 29 (1) (1996) 297–301, https://doi.org/10.1016/0920-5861(95)00295-2.
[15] T. Xing, A. Alvarez-Majmutov, R. Gieleciak, J. Chen, Co-hydroprocessing HTL biocrude from waste biomass with bitumen-derived vacuum gas oil, Energy Fuels 33 (11) (2019) 11135–11144, https://doi.org/10.1021/acs.energyfuels.9b02711.
[16] D.P. Upare, S. Park, M.S. Kim, J. Kim, D. Lee, J. Lee, H. Chang, W. Choi, S. Choi, Y. P. Jeon, Y.K. Park, C.W. Lee, Cobalt promoted Mo/beta zeolite for selective hydrocracking of tetralin and pyrolysis fuel oil into monocyclic aromatic hydrocarbons, J. Ind. Eng. Chem. 35 (2016) 99–107, https://doi.org/10.1016/j.jiec.2015.12.020.
[17] X. Zheng, J. Chang, Y. Fu, One-pot catalytic hydrocracking of diesel distillate and residual oil fractions obtained from bio-oil to gasoline-range hydrocarbon fuel, Fuel 157 (2015) 107–114, https://doi.org/10.1016/j.fuel.2015.05.002.
[18] S. Bezergianni, A. Kalogianni, I.A. Vasalos, Hydrocracking of vacuum gas oil-vegetable oil mixtures for biofuels production, Bioresour. Technol. 100 (12) (2009) 3036–3042, https://doi.org/10.1016/j.biortech.2009.01.018.
[19] S. Bezergianni, A. Dimitriadis, Temperature effect on co-hydroprocessing of heavy gas oil–waste cooking oil mixtures for hybrid diesel production, Fuel 103 (2013) 579–584.
[20] M.S. El-Sawy, S.A. Hanafi, F. Ashour, T.M. Aboul-Fotouh, Co-hydroprocessing and hydrocracking of alternative feed mixture (vacuum gas oil/waste lubricating oil/waste cooking oil) with the aim of producing high quality fuels, Fuel 269 (2020), 117437, https://doi.org/10.1016/j.fuel.2020.117437.
[21] R. Tiwari, B.S. Rana, R. Kumar, D. Verma, R. Kumar, R.K. Joshi, M.O. Garg, A. K. Sinha, Hydrotreating and hydrocracking catalysts for processing of waste soya-oil and refinery-oil mixtures, Catal. Commun. 12 (6) (2011) 559–562, https://doi.org/10.1016/j.catcom.2010.12.008.
[22] N. Bergvall, L. Sandström, F. Weiland, O.G.W. Öhrman, Corefining of fast pyrolysis bio-oil with vacuum residue and vacuum gas oil in a continuous slurry hydrocracking process, Energy Fuels 34 (7) (2020) 8452–8465, https://doi.org/10.1021/acs.energyfuels.0c01322.
[23] K. Sharma, T.H. Pedersen, S.S. Toor, Y. Schuurman, L.A. Rosendahl, Detailed investigation of compatibility of hydrothermal liquefaction derived biocrude oil with fossil fuel for corefining to drop-in biofuels through structural and compositional analysis, ACS Sustain. Chem. Eng. 8 (22) (2020) 8111–8123, https://doi.org/10.1021/acssuschemeng.9b06253.
[24] J. Hoffmann, C.U. Jensen, L.A. Rosendahl, Co-processing potential of HTL bio-crude at petroleum refineries – Part 1: fractional distillation and characterization, Fuel 165 (2016) 526–535, https://doi.org/10.1016/j.fuel.2015.10.094.
[25] D.J. Cookson, B.E. Smith, Determination of structural characteristics of saturates from diesel and kerosine fuels by carbon-13 nuclear magnetic resonance spectrometry, Anal. Chem. 57 (4) (1985) 864–871, https://doi.org/10.1021/ac00281a020.
[26] M. Bouquet, A. Bailleul, Routine method for quantitative 13C n.m.r. spectra editing and providing structural patterns. Application to every kind of petroleum fractions including residues and asphaltenes, Fuel 65 (9) (1986) 1240–1246, https://doi.org/10.1016/0016-2361(86)90236-X.
[27] J. Stihle, D. Uzio, C. Lorentz, N. Charon, J. Ponthus, C. Geantet, Detailed characterization of coal-derived liquids from direct coal liquefaction on supported catalysts, Fuel 95 (2012) 79–87, https://doi.org/10.1016/j.fuel.2011.11.072.
[28] A. Lelevic, V. Souchon, M. Moreaud, C. Lorentz, C. Geantet, Gas chromatography vacuum ultraviolet spectroscopy: a review, J. Sep. Sci. 43 (1) (2020) 150–173, https://doi.org/10.1002/jssc.201900770.

[29] A. Lelevic, V. Souchon, C. Geantet, C. Lorentz, M. Moreaud, Quantitative performance of forward fill/flush differential flow modulation for comprehensive two-dimensional gas chromatography, J. Chromatogr. A 1626 (2020), 461342, https://doi.org/10.1016/j.chroma.2020.461342.
[30] F. de Miguel Mercader, M.J. Groeneveld, S. Kersten, C. Geantet, G. Toussaint, N. Way, C.J. Schaverien, K. Hogendoorn, Hydrodeoxygenation of pyrolysis oil fractions: process understanding and quality assessment through co-processing in refinery units, Energy Environ. Sci. 4 (3) (2011) 985–997, https://doi.org/10.1039/C0EE00523A.
[31] R.H. Venderbosch, H.J. Heeres, Pyrolysis oil stabilization by catalytic hydrotreatment, in: B.A. dos Santos (Ed.), Biofuel's Engineering Process Technology, Marco, 2011, pp. 385–410.
[32] E. Heeres, A. Ardiyanti, A. Kloekhorst, Y. Wng, S.A. Khromova, V. Yakovlev, et al., Novel Ni- based catalysts for the hydrotreatment of fast pyrolysis oil, in: M. Garcia-Perez, D. Meier, R. Ocone, P. de Wild (Eds.), BioEnergy IV: Innovations in Biomass Conversion for Heat, Power, Fuels and Chemicals, ECI Symposium Series, 2013.
[33] P. Álvarez, B. Browning, T. Jansen, M. Lacroix, C. Geantet, I. Pitault, M. Tayakout-Fayolle, Modeling of atmospheric and vacuum petroleum residue hydroconversion in a slurry semi-batch reactor: study of hydrogen consumption, Fuel Process. Technol. 185 (2019) 68–78, https://doi.org/10.1016/j.fuproc.2018.11.016.
[34] A. Corma, A. Martinez, V. Martinezsoria, J.B. Monton, Hydrocracking of vacuum gasoil on the novel mesoporous MCM-41 aluminosilicate catalyst, J. Catal. 153 (1) (1995) 25–31, https://doi.org/10.1006/jcat.1995.1104.
[35] P. Raybaud, H. Toulhoat, Catalysis by Transition Metal Sulphides: From Molecular Theory to Industrial Application, TECHNIP, 2013.
[36] R. Henry, M. Tayakout-Fayolle, P. Afanasiev, C. Lorentz, G. Lapisardi, G. Pirngruber, Vacuum gas oil hydrocracking performance of bifunctional Mo/Y zeolite catalysts in a semi-batch reactor, Catal. Today 220–222 (2014) 159–167, https://doi.org/10.1016/j.cattod.2013.06.024.
[37] J. Weitkamp, Catalytic hydrocracking—mechanisms and versatility of the process, ChemCatChem 4 (3) (2012) 292–306, https://doi.org/10.1002/cctc.201100315.
[38] T. Zhang, C. Leyva, G. Froment, J. Martinis, Vacuum gas oil hydrocracking on NiMo/USY zeolite catalysts. experimental study and kinetic modeling, Ind. Eng. Chem. Res. 54 (2015) 858–868, https://doi.org/10.1021/ie503567b.
[39] H. Kumar, G.F. Froment, Mechanistic kinetic modeling of the hydrocracking of complex feedstocks, such as vacuum gas oils, Ind. Eng. Chem. Res. 46 (18) (2007) 5881–5897, https://doi.org/10.1021/ie0704290.
[40] B. Browning, P. Afanasiev, I. Pitault, F. Couenne, M. Tayakout-Fayolle, Detailed kinetic modelling of vacuum gas oil hydrocracking using bifunctional catalyst: a distribution approach, Chem. Eng. J. 284 (2016) 270–284, https://doi.org/10.1016/j.cej.2015.08.126.
[41] P.J. Becker, B. Celse, D. Guillaume, V. Costa, L. Bertier, E. Guillon, G. Pirngruber, A continuous lumping model for hydrocracking on a zeolite catalysts: model development and parameter identification, Fuel 164 (2016) 73–82, https://doi.org/10.1016/j.fuel.2015.09.057.
[42] S. Sadighi, Comparison of lumping approaches to predict the product yield in a dual bed VGO hydrocracker, Int. J. Chem. React. Eng. 9 (2011) (janv.).
[43] A.R. Moghadassi, N. Amini, O. Fadavi, M. Bahmani, The application of the discrete lumped kinetic approach for the modeling of a vacuum gas oil hydrocracker unit, Pet. Sci. Technol. 29 (23) (2011) 2416–2424, https://doi.org/10.1080/10916461003699150.
[44] G. Valavarasu, B. Sairam, Hydrocracking of vacuum gas oil: conversion, product yields, and product quality over an industrial hydrocracking catalyst system, Pet. Sci. Technol. 31 (6) (2013) 551–562, https://doi.org/10.1080/10916466.2010.516296.
[45] A. Alvarez-Majmutov, S. Badoga, J. Chen, J. Monnier, Y. Zhang, Co-processing of deoxygenated pyrolysis bio-oil with vacuum gas oil through hydrocracking, Energy Fuels 35 (12) (2021) 9983–9993, https://doi.org/10.1021/acs.energyfuels.1c00822.
[46] Y. Romero, F. Richard, S. Brunet, Hydrodeoxygenation of 2-ethylphenol as a model compound of bio-crude over sulfided Mo-based catalysts: promoting effect and reaction mechanism, Appl. Catal. B: Environ. 98 (3) (2010) 213–223, https://doi.org/10.1016/j.apcatb.2010.05.031.
[47] V. Bui, D. Laurenti, P. Afanasiev, C. Geantet, Hydrodeoxygenation of guaiacol with CoMo catalysts. Part I: promoting effect of cobalt on HDO selectivity and activity, Appl. Catal. B: Environ. 101 (2011) 239–245, https://doi.org/10.1016/j.apcatb.2010.10.025.
[48] K. Pstrowska, J. Walendziewski, R. Luzny, M. Stolarski, Hydroprocessing of rapeseed pyrolysis bio-oil over $NiMo/Al_2O_3$ catalyst, Catal. Today 223 (2014) 54–65, https://doi.org/10.1016/j.cattod.2013.10.066.
[49] D.C. Elliott, Historical developments in hydroprocessing bio-oils, Energy Fuels 21 (3) (2007) 1792–1815, https://doi.org/10.1021/ef070044u.
[50] L. Mahé, T. Dutriez, M. Courtiade, D. Thiébaut, H. Dulot, F. Bertoncini, Global approach for the selection of high temperature comprehensive two-dimensional gas chromatography experimental conditions and quantitative analysis in regards to sulfur-containing compounds in heavy petroleum cuts, J. Chromatogr. A 1218 (3) (2011) 534–544, https://doi.org/10.1016/j.chroma.2010.11.065.
[51] A. Pinheiro, D. Hudebine, N. Dupassieux, C. Geantet, Impact of oxygenated compounds from lignocellulosic biomass pyrolysis oils on gas oil hydrotreatment, Energy Fuels 23 (2) (2009) 1007–1014, https://doi.org/10.1021/ef800507z.
[52] N. Thegarid, G. Fogassy, Y. Schuurman, C. Mirodatos, S. Stefanidis, E.F. Iliopoulou, K. Kalogiannis, A.A. Lappas, Second-generation biofuels by co-processing catalytic pyrolysis oil in FCC units, Appl. Catal. B: Environ. 145 (2014) 161–166, https://doi.org/10.1016/j.apcatb.2013.01.019.